

**Figure 2A.** Ingenuity analysis of the top pathways affected in differentially expressed genes among 129 bladder cancer and 17 normal tissue samples (Cohort B). Y-axis is an inverse indication of p-value or significance. (A) Gene networks involved in “cell cycle, gene expression and cell death” (B), and “cell morphology, cellular function and maintenance and cell death” (C), generated by IPA for differentially expressed genes between bladder cancer and normal tissue. The selected scoring method was Fisher’s exact test p-value. The threshold value was set at  $p = 0.05$ . Red symbols are assigned for upregulated and green for downregulated genes. Node shape corresponds to the functional role of molecules as shown in the legend. Direct or indirect interactions are shown by complete or dashed lines.

the samples with constant chromosome location. These results were further fitted using Fourier series (Eqn. 3). The result for chromosome 1 is presented in Figure S6. We further analyzed the data by calculating the confidence intervals at the 95% level, the first and second derivatives, as well as the integral of the fitted data. An interesting observation was that the derivatives of the fitted data manifested oscillatory behavior. In addition, we present the results of our analysis for chromosome X in Figure S7. All remaining chromosomes were analyzed accordingly (data not shown due to space limitations).

Our analysis proceeded with the consideration of chromosomes vs. gene expression. Similarly, we performed k-means clustering analysis (Fig. S8) for the first 10 samples. The remaining 130 samples were clustered accordingly. Simulations of this dimension of the cube were succeeded with Fourier series as mentioned in the “Materials and Methods” section and Equation 3. The result is presented in Figure S9 with indicative diagrams of our analysis. The cubical matrix that was implemented is a very complex structure, which eventually manifests nonlinear dynamics with respect to gene expression.

*Gene ontology (GO) enrichment analysis.* Gene expression was further investigated using GO enrichment. Function distribution along chromosomes is presented in Figure S10. Chromosome 5 presented more functions compared with the other chromosomes. GO enrichment was not proportional to the chromosome size, since the largest chromosome 1 presented 35 significant functions. All the significant gene functions per chromosome are presented in Table 3.

## Discussion

Several studies have focused on the expression profiling of bladder cancer using microarrays.<sup>12-21</sup> In the present study, the bladder

cancer cases were carefully selected in order to obtain at least one pair from each of the following groups: T1-grade 2, T1-grade 3 and T2/T3-grade 3. Furthermore, in our pooled microarray analysis, a wide range of data from publicly available microarray data sets was included, increasing the total number to 129 bladder cancer and 17 control samples. Statistical analysis results were obtained from our previous works,<sup>7,35</sup> and the same collection of genes was used. All conclusions and further analyses were based on the differential gene expression reported. The main difference is that this same data set was further divided according to the chromosomal location of each identified gene.

We performed IPA for two separate cohorts (A and B) and constructed chromosome correlation maps for all bladder tumors in order to visualize co-deregulated genes along the chromosomes. Network analysis manifested two distinct signaling pathways, the glucocorticoid receptor (GR) and NF $\kappa$ B signaling pathway. These pathways are known to be antagonistic, since the second is responsible for the inflammatory response while the first for the anti-inflammatory one.<sup>22</sup> It has been reported that tumors of the urinary tract are not considered to be hormone-dependent, yet it has been shown that nuclear receptors participate in urinary tumor ontogenesis.<sup>23</sup> Also, there are no reports connecting bladder cancer to NF $\kappa$ B. The finding that genes that possibly participate in the progression of the tumor are related to the NF $\kappa$ B signaling pathway is presented for the first time.

The mean value of the DE genes in tumor groups vs. control samples on chromosome 1 was positive, implying that these genes are upregulated. The most interesting case, however, was the appearance of *CDC20*, also previously reported to be significantly overexpressed in bladder cancer.<sup>7</sup> Also, *GPREL1* (chromosome 4) and *HCCS* (chromosome X) were the most active genes among all tumor samples. *CDC20* has been previously reported to act as a potent TP53 target and is a putative therapeutic target gene.<sup>24</sup>

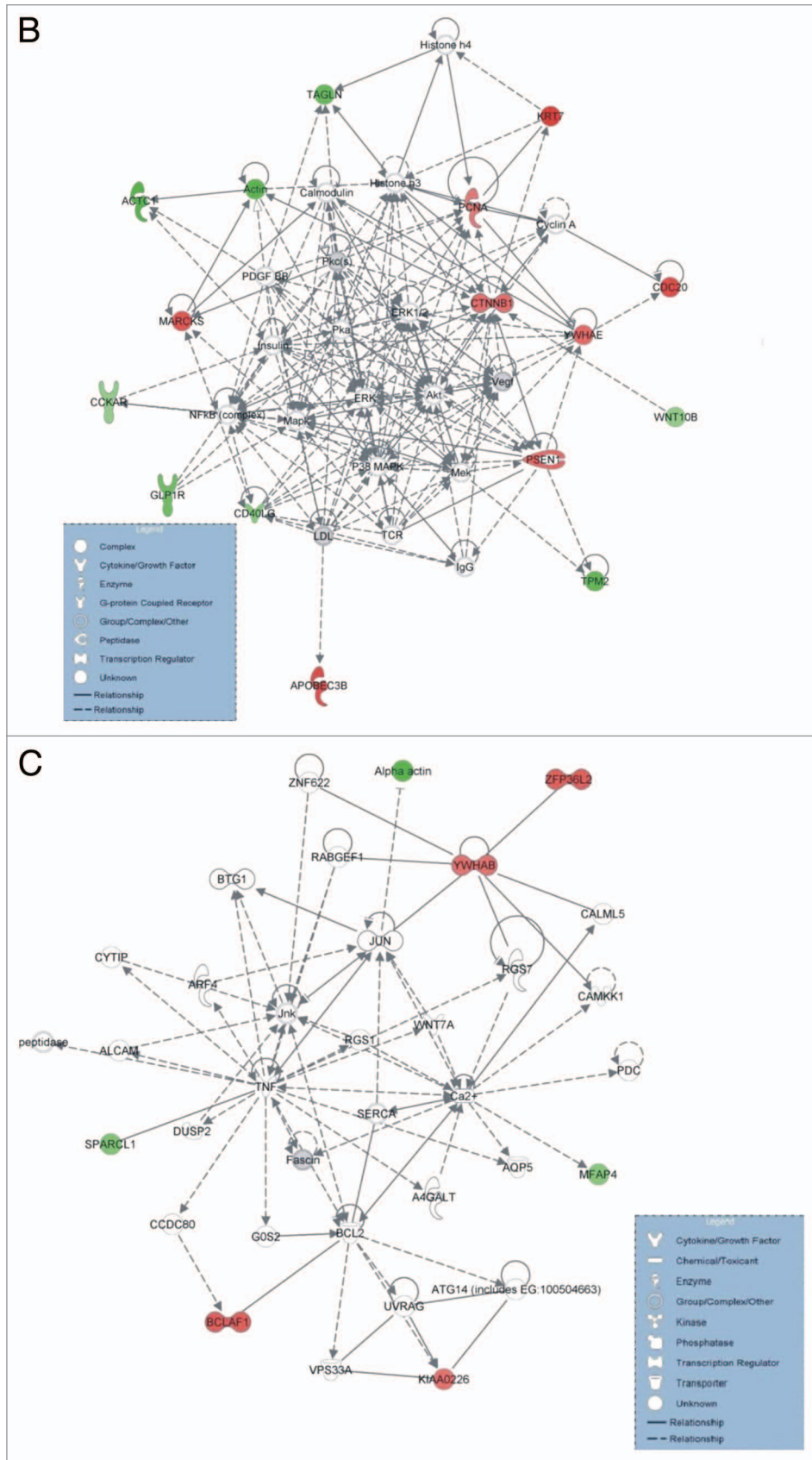
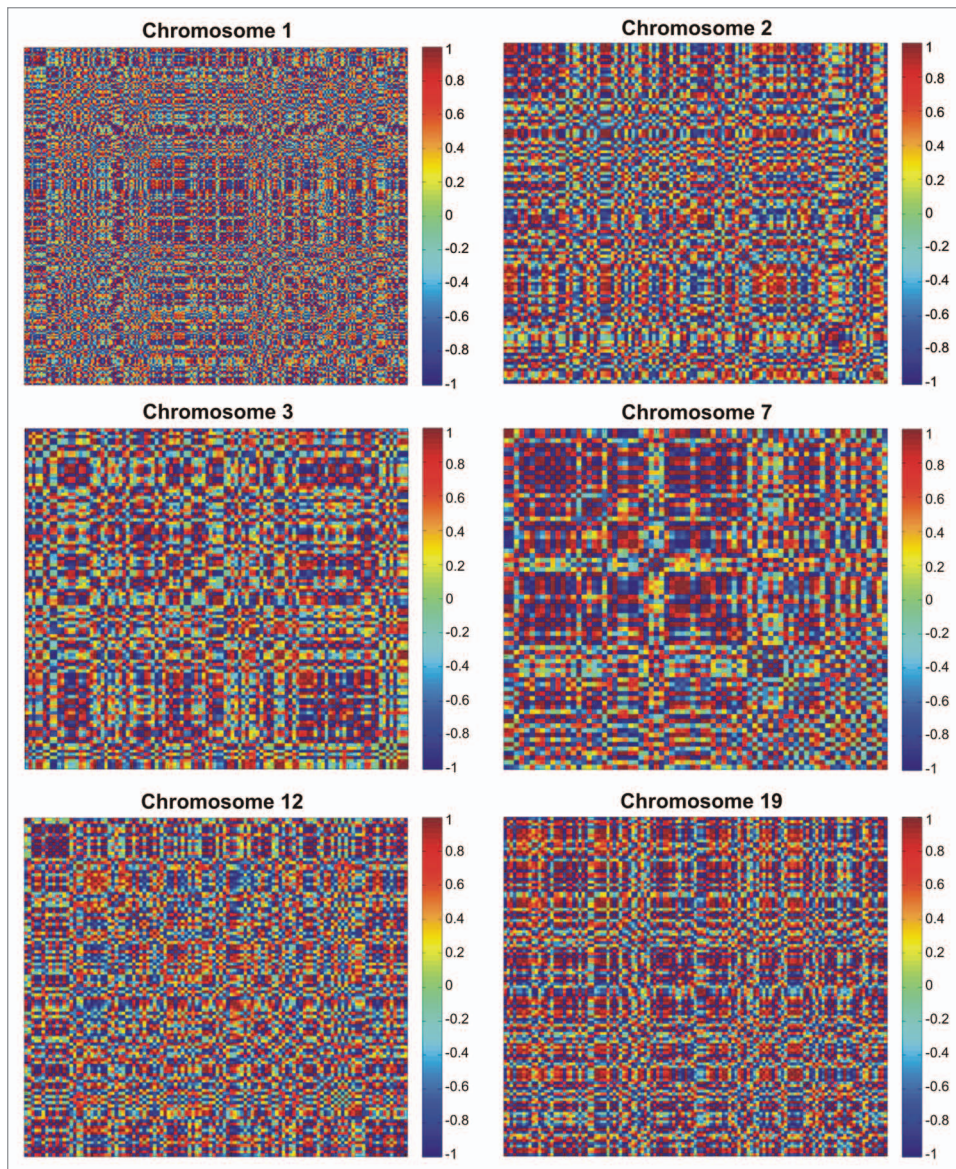


Figure 2B and C. For figure legend, see page 6.



**Figure 3.** Chromosome correlation maps of the DE genes between T $\alpha$ -grade 1 tumors and control samples, on chromosomes 1, 2, 3, 7, 12 and 19. The X and Y axes represent the individual genes that were differentially expressed between control and Ta-grade 1 tumors.

Significantly co-expressed genes along chromosomes 1, 2, 3, 7, 12 and 19 appeared among the tumor subgroups with respect to the control samples. To our knowledge, this is the first report that indicates such gene expression correlations in bladder cancer. Since this was a first indication of gene regulatory mechanism, we wished to ascertain whether gene expression could be simulated. It is known that the existence of correlation (gene co-expression) does not automatically mean causation. This was confirmed to be true by successful simulation. Interestingly, when we separated the genes based on their chromosome location, they could be fitted with a third-degree polynomial, hinting toward the existence of linear correlation regulatory mechanisms. This suggests that gene expression falls into a conserved mechanism of expression. The simulation revealed that among different tumor samples,

the genes on the same chromosomes were expressed in a similar manner.

Likewise, we constructed chromosome correlation maps for the T $\alpha$ -grade 2 tumors and found that chromosome-based gene expression manifested diverse correlation patterns. Thus, it was not a strong indication of correlation in this type of tumor. As in the case of T $\alpha$ -grade 1 tumors, expression data simulation also showed an excellent fit ( $0.7 < R^2 < 0.9$ ). These two cases suggest that correlation possibly also meant causation for these tumor types.

Next, we constructed chromosome correlation maps for the control samples alone in order to examine whether the correlations had to do only with relative ratios of tumors vs. the controls. Our analysis revealed chromosomal domains of gene co-expression for the control samples as well. Fitting attempts also showed that gene expression data could be simulated using polynomial functions, and again correlation hinted toward causation in normal tissue samples. To the best of our knowledge, this is the first time that microarray data are analyzed in such a way.

Despite the interesting type of mechanisms observed so far, especially in T $\alpha$ -grade 1 and T $\alpha$ -grade 2 tumors, we still wished to investigate whether such correlations appeared due to the small sample size that was used in the simulation procedures. Therefore, the next step was to perform the analysis in the complete sample size, in an attempt to gain insight into the whole picture

of chromosome-based gene expression. For this purpose, we created the “gene cube.” The idea was that similarly regulated genes should manifest similar dynamics. Interestingly, it appeared that experimental data could be fitted with transformations, indicating that there are, at least in part, linear dynamics governing simplifications of the system described. New findings of molecular markers have been reported in the past in similar studies, using bioinformatics tools to identify gene expression signatures.<sup>25,26</sup> Thus the dynamics of chromosomal gene expression is of high significance in tumor biology. From our analysis, it was evident that gene expression has partly linear dynamics.

Genes on chromosomes 1 and 12 manifested functions related to embryonic development. The role of developmental genes in urothelial carcinomas was also previously reported.<sup>23,27</sup>

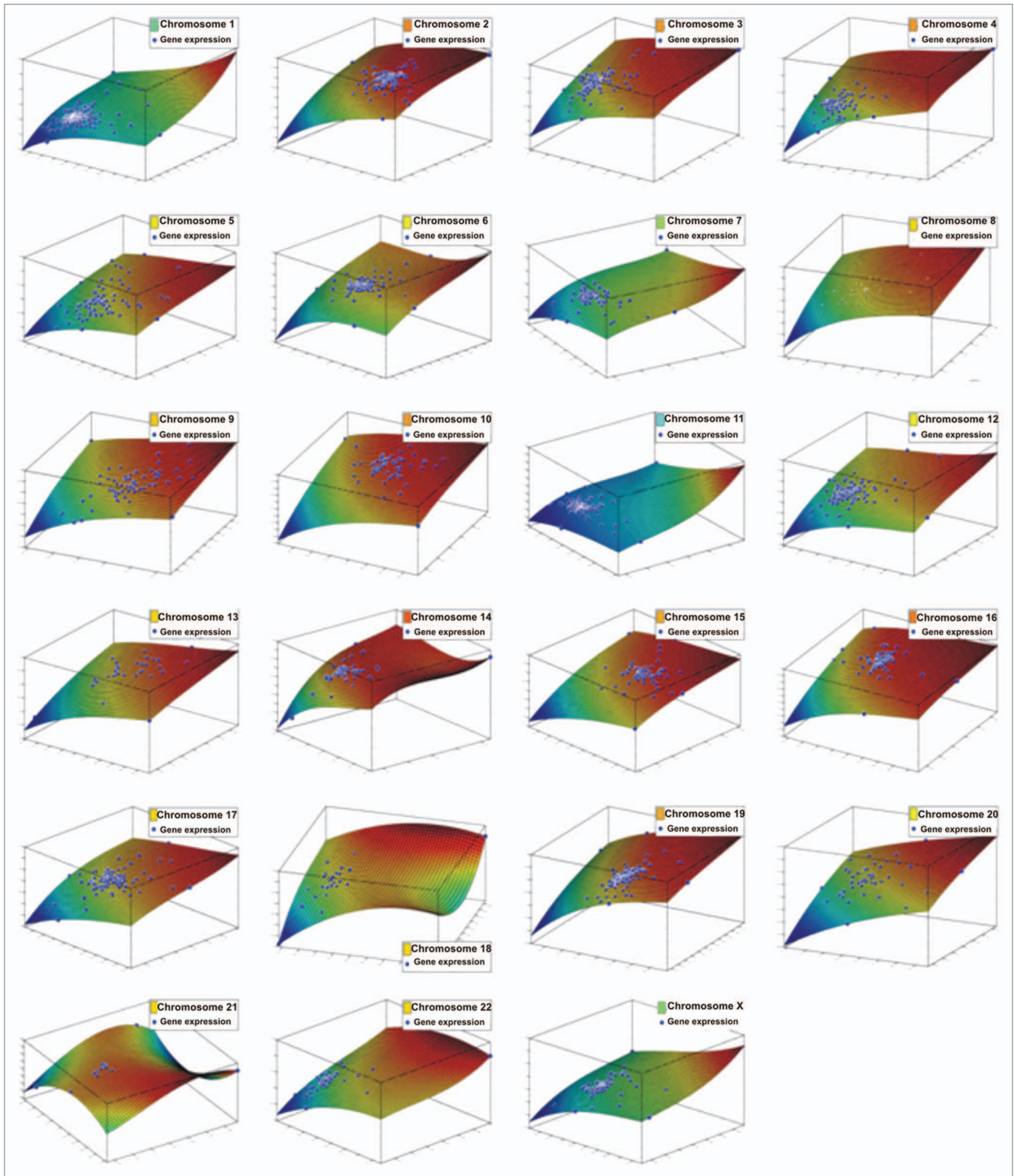


**Figure 4.** Simulations of the DE genes with respect to their chromosome location, among T $\alpha$ -grade 1 tumors and control samples. Each chromosome is presented separately. All genes could be simulated with a third-degree polynomial and  $R^2 > 0.99$ . Axes represent gene expression values of the  $\log_2$  ratio of the Ta-grade 1 tumors over control samples, where each axis represents one sample from the tumor subtype (Ta-grade 1 tumor group consisted of three samples).

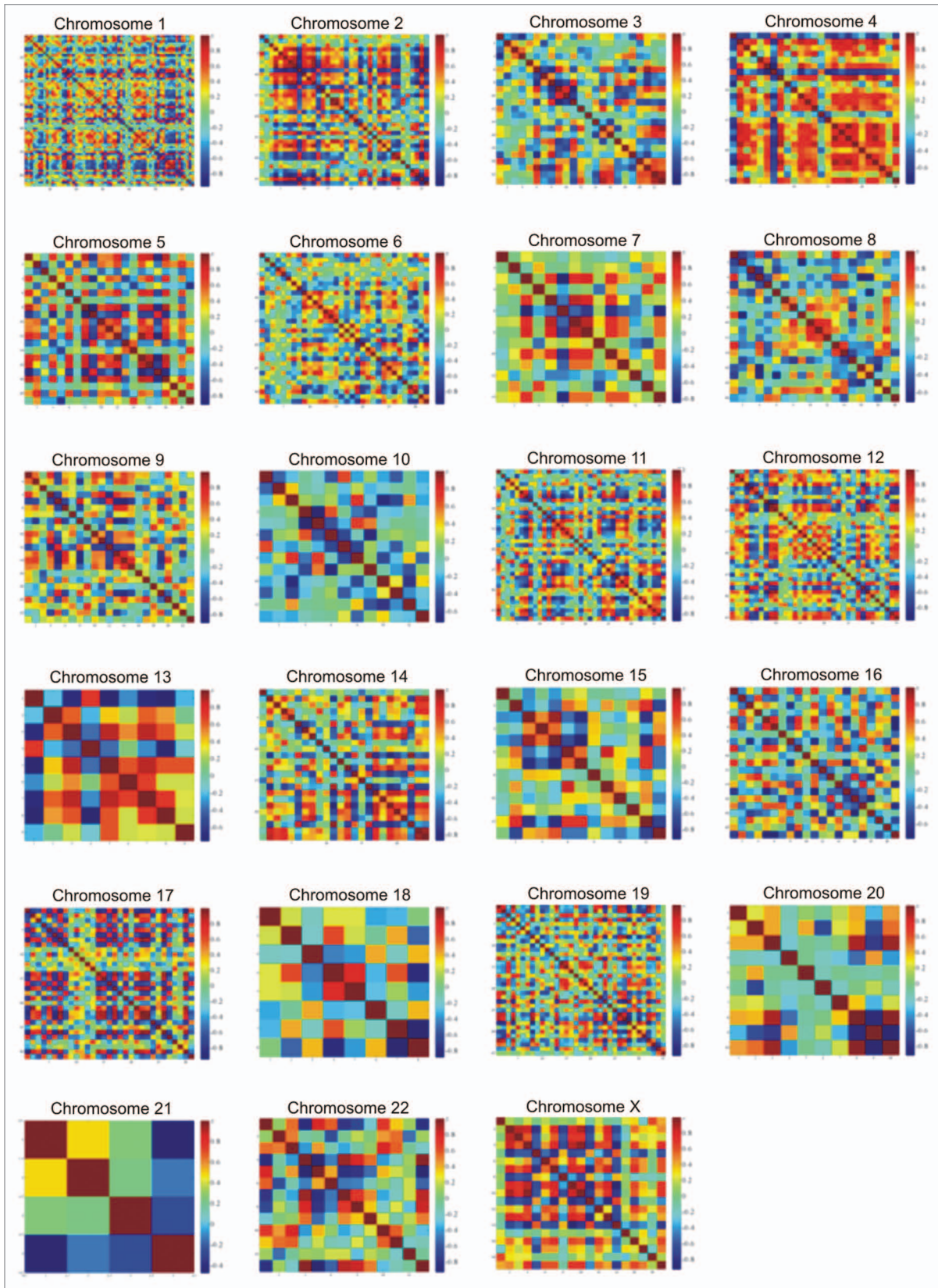


**Figure 5.** Chromosome correlation maps for T $\alpha$ -grade 2 tumors allow visualization of co-expressed genes along all chromosomes.

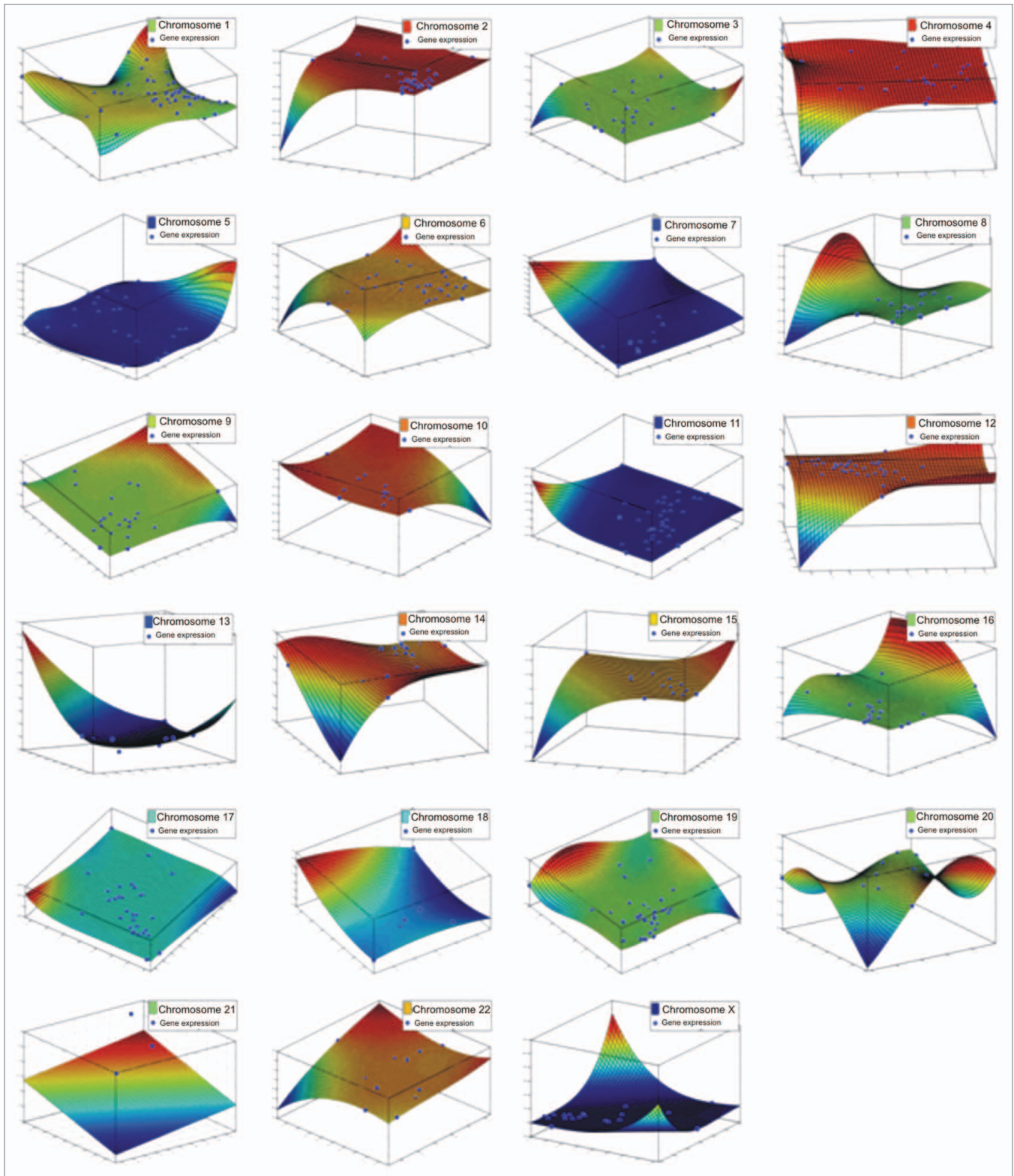


**Figure 6.** Simulations of the DE genes with respect to their chromosome location, among T $\alpha$ -grade 2 tumors and control samples. Each chromosome is presented separately. All genes could be simulated with a third degree polynomial and  $R^2 > 0.99$ . Axes represent gene expression values of the  $\log_2$  ratio of the Ta-grade 2 tumors over control samples, where each axis represents one sample from the tumor subtype. Ta-grade 2 consisted of 12 samples in total. The figure includes representative fittings of the samples GSM2526\_Ta gr2, GSM2536\_Ta gr2 and GSM2507\_Ta gr2 for each chromosome, respectively.

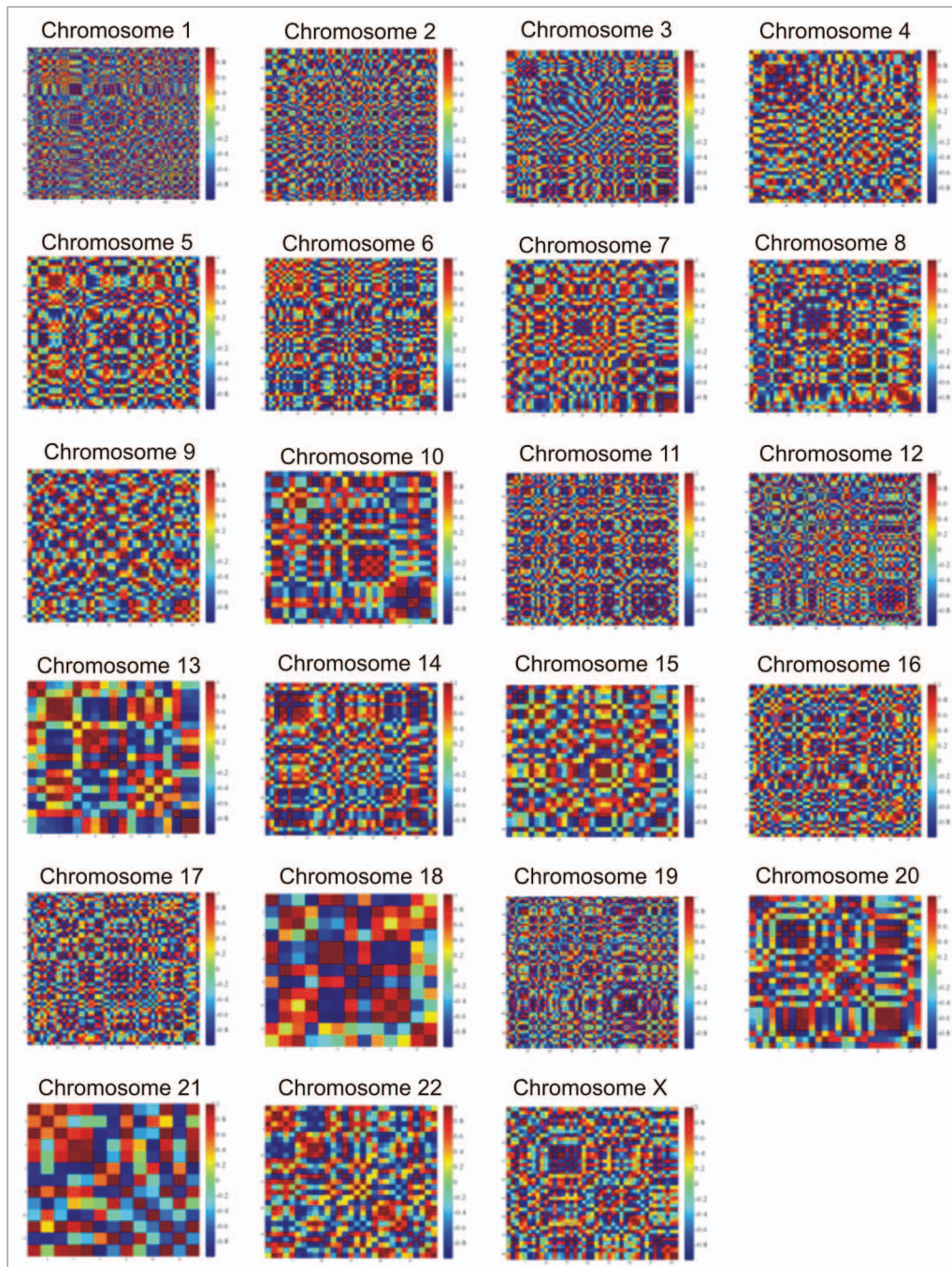


**Figure 7.** Chromosome correlation maps for T1-grade 2 tumors allow visualization of co-expressed genes along all chromosomes. The X and Y axes represent the individual genes that were differentially expressed between control samples and T1-grade 2 tumors.

In particular, the genes related to this function were IL10 and VCAM1. VCAM1 has been reported to be upregulated in bladder carcinomas.<sup>28</sup> On the other hand, genes on chromosome 12 were LRP6, WNT1 and WNT10B. There are no reports linking *LRP6*, *WNT1* and *WNT10B* with bladder cancer. Genes on chromosome 10 were related to the WNT receptor signaling pathway (*BAMBI*, *BTRC*, *DKK1*, *FBXW4*, *FRAT1*, *FRAT2*, *FZD8*, *HHEX*, *LDB1*, *SFRP5*, *TCF7L2* and *WNT8B*). *BAMBI* has been linked with high-grade bladder carcinomas through epigenetic

silencing.<sup>29</sup> Also, *TCF7L2* has been reported to play a role in the WNT signaling pathway, where its inhibition seems to lead to G<sub>1</sub> arrest and growth inhibition of the bladder cancer. Genes on chromosome 4 and 9 participated in chemokine regulation. In particular, on chromosome 4, a large CXCL family is represented, including CXCL10, CXCL11, CXCL13, CXCL3, CXCL5, CXCL6, CXCL9 and IL8, PF4 and PPBP. The CXCL family of chemokines has been reported to participate in the microenvironment of bladder carcinoma.<sup>30</sup> IL8 has also been reported to

participate in bladder cancer.<sup>31</sup> *GHR*, *IL12B* and *PRLR* on chromosome 5 presented functions related to JAK2 kinase activity. So far, there are no reports connecting these genes with bladder tumors. Yet, it has been reported that the JAK/STAT participates in the inflammatory mechanisms of urinary bladder, relating it to the oncogenetic mechanisms of the disease.<sup>32</sup> Finally, on chromosome 22, MAPK1, MAPK11 and MAPK12 participate in the MAPK pathway. Interestingly, it has been reported that the inhibition of MAPK and NFκB signaling pathways inhibits growth and induces apoptosis of bladder tumor cells.<sup>33,34</sup>

Our data support the hypothesis that gene expression signatures can provide further information on gene regulatory mechanisms, based on chromosomal correlations of gene expression. The “Gene Cube” proved that gene expression has partly linear dynamics. Future research should focus on the investigation of these correlations in gene expression.

## Materials and Methods

**Strategy of the study.** In the first part, we performed microarray experimentation as previously described in detail<sup>7,35</sup> (Cohort A). The tumor samples were divided into three groups, as follows: T1-grade 2, T1-grade 3 and T2/T3-grade 3. All raw microarray data were MIAME compliant and uploaded on the GEO database (GSE27448).<sup>7</sup> The study was approved by the institutional review board of the University of Crete. For further data analysis, the Matlab<sup>®</sup> software was used.

In the second part, we extracted raw microarray expression data from 4 GEO data sets: (1) GSE89;<sup>13</sup> (2) GSE3167;<sup>14</sup> (3) GSE7476;<sup>36</sup> (4) GSE12630,<sup>37</sup> and incorporated them in our analysis, as previously described in detail.<sup>7</sup> All microarray data were background corrected and cross-normalized using a quantile algorithm.<sup>38-40</sup> In total, our pooled microarray analysis comprised 17 normal tissues and 129 bladder cancer samples (Cohort B).

All samples used from each data set with their respective GSM accession number, and detailed information regarding each sample’s tumor type has been previously described in detail.<sup>7</sup>

**Network analysis.** The co-deregulated genes among bladder cancer samples were investigated for network interrelation using the Ingenuity Pathways Analysis (IPA) software (www.ingenuity.com). The DE genes between cancer and normal tissue were used to generate a set of networks with a maximum network size of 35 genes/proteins. The median log<sub>2</sub> fold change value was used for analysis.

**Microarray data statistics.** First, we compared all the bladder cancer vs. all the normal tissue samples, entailing all bias by comparing them as unified groups. This analysis provided us with the co-DE genes. Second, we separated the 129 bladder cancer samples into 11 groups: (1) Tα-grade 1 tumors vs. controls; (2) Tα-grade 2 tumors vs. controls; (3) Tα-grade 3 tumors vs. controls; (4) T1-grade 2 tumors vs. controls; (5) T1-grade 3 tumors vs. controls; (6) T1-grade 2 and T1-grade 3 tumors vs. controls; (7) T1-grade 2, T1-grade 3 and T1-grade 4 tumors vs. controls; (8) group A<sup>15</sup> vs. controls; (9) group B<sup>15</sup> vs. controls; (10) group C<sup>15</sup> vs. controls; (11) metastatic tumors vs. controls. Each group was compared against all control samples. The false

discovery rate (FDR) was 8.6% for p < 0.05, calculated as previously described.<sup>41-43</sup>

**Cluster analysis.** K-means clustering with squared Euclidean as a metric distance was used to partition the gene expression profiles throughout the experimental setups.<sup>44</sup> The procedure was repeated 100 times, each with a new set of initial cluster centroid positions. The predictive power of the k-means algorithm was estimated using a figure of merit (FOM).<sup>45</sup> A FOM value vs. number of clusters was computed by removing each sample in turn from the data set, clustering genes based on the remaining data and calculating the fit of the withheld sample to the clustering pattern obtained from the other samples.

**Chromosome mapping and linear correlations.** Since consecutive genes are often similarly expressed, we mapped the genes on chromosome regions and identified their correlations through their chromosomal location.<sup>10</sup> The Gene Ontology Tree Machine, WebGestalt web-tool (Vanderbilt University, The Netherlands, <http://bioinfo.vanderbilt.edu/gotm/>)<sup>46</sup> and the Matlab<sup>®</sup> (The Mathworks Inc.) computing environments were used. Linear correlations were calculated using Pearson’s correlation coefficient. The value  $R^2 > 0.9$  was set as a threshold for statistical significance.

**Gene ontology (GO) enrichment.** GO analysis was applied to highlight the different functionalities among the experimental setups. For each chromosomal gene set formed, statistical analysis of GO term overrepresentation was performed against the common gene set, which was utilized as a reference set.<sup>47,48</sup> The chosen approach was the parent-child-union method.<sup>49</sup> Overrepresentation analysis (ORA) was performed with the publicly available Ontologizer 2.0 tool<sup>50</sup> using GO terms definitions and associations between genes and GO downloaded from the Gene Ontology consortium.<sup>51</sup> The threshold for statistical significance was set to < 0.01 using Bonferroni correction.

**Mathematical modeling and simulations.** Simulations were performed using Matlab<sup>®</sup>. For fitting purposes we used polynomial equations for 2D (Eqn. 1) and for 3D (Eqn. 2):

**Equation 1:**

$$f(x) = a_0 + a_1x^n + a_2x^{n-1} + \dots + a_nx$$

**Equation 2:**

$$f(x,y) = a_0 + a_1x^n + a_2x^{n-1}y + a_3x^{n-2}y^2 + a_4x^{n-3}y^3 + \dots + a_5x^3y^{n-3} + a_6x^2y^{n-2} + a_7xy^{n-1} + a_8y^n$$

Fourier series model as in Equation 3:

$$f(x) = a_0 + \sum_{i=1}^n (a_i \cos(mwx) + b_i \sin(mwx))$$

Sum of sin functions as in Equation 4:

$$f(x) = \sum_{i=1}^n a_i \sin(b_i x + c_i)$$

Fitting algorithm finds the coefficients of a polynomial  $f(x)$  of degree  $n$  that fits the data,  $f[x(i)]$  to  $y(i)$ , in a least squares sense. The result  $p$  is a row vector of length  $n+1$  containing the polynomial coefficients in descending powers as shown in Equations 1 and 2.

On the other hand the Fourier series is a sum of sine and cosine functions that describes a periodic signal (Eqn. 3). It is represented in either the trigonometric form or the exponential

**Table 3.** Selected GO terms of chromosomal-based gene expression

GO analysis		
ID	Name	p-value (Adj)
<b>chromosome 1</b>		
GO:0060669	embryonic placenta morphogenesis	0.0045
GO:0005839	proteasome core complex	0.0014
GO:0005031	tumor necrosis factor receptor activity	0.0067
<b>chromosome 2</b>		
GO:0009952	anterior/posterior pattern formation	0.0018
GO:0007350	blastoderm segmentation	0.0064
GO:0048468	cell development	0.0071
GO:0048562	embryonic organ morphogenesis	0.0025
GO:0048706	embryonic skeletal system development	0.0062
GO:0005152	interleukin-1 receptor antagonist activity	0.0052
GO:0004918	interleukin-8 receptor activity	0.0052
<b>chromosome 3</b>		
GO:0016493	C-C chemokine receptor activity	4.71E-05
GO:0071425	hemopoietic stem cell proliferation	0.0043
<b>chromosome 4</b>		
GO:0001525	Angiogenesis	0.0052
GO:0008009	chemokine activity	2.99E-07
GO:0008083	growth factor activity	0.0008
GO:0005134	interleukin-2 receptor binding	0.0059
GO:0051781	positive regulation of cell division	0.0001
GO:0045741	positive regulation of epidermal growth factor receptor activity	0.0008
GO:0050729	positive regulation of inflammatory response	0.0027
GO:0045410	positive regulation of interleukin-6 biosynthetic process	0.0003
GO:0045840	positive regulation of mitosis	0.0061
GO:0034105	positive regulation of tissue remodeling	0.0087
GO:0008202	steroid metabolic process	0.0065
<b>chromosome 5</b>		
GO:0042977	activation of JAK2 kinase activity	0.0010
GO:0035240	dopamine binding	0.0020
GO:0008083	growth factor activity	0.0048
GO:0070851	growth factor receptor binding	0.0056
GO:0005138	interleukin-6 receptor binding	0.0068
GO:0004923	leukemia inhibitory factor receptor activity	0.0023

The terms were considered significant if they obtained an adjusted p-value < 0.01.

form. The algorithm used in the present work used the trigonometric Fourier series form, where  $a_0$  models a constant (intercept) term in the data and is associated with the  $i = 0$  cosine term,  $w$  is the fundamental frequency of the signal,  $n$  is the number of terms (harmonics) in the series, and  $1 \leq n \leq 8$ .

**Table 3.** Selected GO terms of chromosomal-based gene expression (continued)

GO analysis		
ID	Name	p-value (Adj)
<b>chromosome 6</b>		
GO:0060333	interferon-gamma-mediated signaling pathway	1.78E-09
GO:0046415	urate metabolic process	0.0094
GO:0001570	vasculogenesis	0.0089
<b>chromosome 7</b>		
GO:0035425	autocrine signaling	0.0022
GO:0060571	morphogenesis of an epithelial fold	0.0072
GO:0045765	regulation of angiogenesis	0.0038
<b>chromosome 9</b>		
GO:0005125	cytokine activity	4.39E-05
<b>chromosome 10</b>		
GO:0005739	mitochondrion	0.0096
GO:0016055	Wnt receptor signaling pathway	0.0078
<b>chromosome 12</b>		
GO:0031076	embryonic camera-type eye development	0.0071
GO:0048048	embryonic eye morphogenesis	0.0051
<b>chromosome 16</b>		
GO:0006264	mitochondrial DNA replication	0.0068
GO:0005759	mitochondrial matrix	0.0060
GO:0010834	telomere maintenance via telomere shortening	0.0068
<b>chromosome 17</b>		
GO:0008009	chemokine activity	5.09E-05
<b>chromosome 21</b>		
GO:0004904	interferon receptor activity	0.0004
<b>chromosome 22</b>		
GO:0004707	MAP kinase activity	0.0007
<b>chromosome X</b>		
GO:0004896	cytokine receptor activity	0.0055

The terms were considered significant if they obtained an adjusted p-value < 0.01.

#### Disclosure of Potential Conflicts of Interest

No potential conflicts of interest were disclosed.

#### Author's Contributions

G.I.L., A.Z. designed and supervised the study, performed the experimental procedures and data interpretation. A.Z. and G.I.L. prepared and submitted the manuscript. M.A., D.D., D.A. and S.V. read and approved the manuscript.

#### Supplemental Materials

Supplemental materials may be found here: [www.landesbioscience.com/journals/cc/article/24673](http://www.landesbioscience.com/journals/cc/article/24673)

## References

- Alizadeh AA, Eisen MB, Davis RE, Ma C, Lossos IS, Rosenwald A, et al. Distinct types of diffuse large B-cell lymphoma identified by gene expression profiling. *Nature* 2000; 403:503-11; PMID:10676951; <http://dx.doi.org/10.1038/35000501>
- Golub TR, Slonim DK, Tamayo P, Huard C, Gaasenbeek M, Mesirov JP, et al. Molecular classification of cancer: class discovery and class prediction by gene expression monitoring. *Science* 1999; 286:531-7; PMID:10521349; <http://dx.doi.org/10.1126/science.286.5439.531>
- Perou CM, Sørli T, Eisen MB, van de Rijn M, Jeffrey SS, Rees CA, et al. Molecular portraits of human breast tumours. *Nature* 2000; 406:747-52; PMID:10963602; <http://dx.doi.org/10.1038/35021093>
- Ross DT, Scherf U, Eisen MB, Perou CM, Rees C, Spellman P, et al. Systematic variation in gene expression patterns in human cancer cell lines. *Nat Genet* 2000; 24:227-35; PMID:10700174; <http://dx.doi.org/10.1038/73432>
- Sørli T, Perou CM, Tibshirani R, Aas T, Geisler S, Johnsen H, et al. Gene expression patterns of breast carcinomas distinguish tumor subclasses with clinical implications. *Proc Natl Acad Sci USA* 2001; 98:10869-74; PMID:11553815; <http://dx.doi.org/10.1073/pnas.191367098>
- Takahashi M, Rhodes DR, Furge KA, Kanayama H, Kagawa S, Haab BB, et al. Gene expression profiling of clear cell renal cell carcinoma: gene identification and prognostic classification. *Proc Natl Acad Sci USA* 2001; 98:9754-9; PMID:11493696; <http://dx.doi.org/10.1073/pnas.171209998>
- Zaravinos A, Lambrou GI, Boulalas I, Delakas D, Spandidos DA. Identification of common differentially expressed genes in urinary bladder cancer. *PLoS ONE* 2011; 6:e18135; PMID:21483740; <http://dx.doi.org/10.1371/journal.pone.0018135>
- de la Fuente A. From 'differential expression' to 'differential networking' - identification of dysfunctional regulatory networks in diseases. *Trends Genet* 2010; 26:326-33; PMID:20570387; <http://dx.doi.org/10.1016/j.tig.2010.05.001>
- Lambrou GI, Zaravinos A, Adamaki M, Spandidos DA, Tzortzidou-Stathopoulou F, Vlachopoulos S. Pathway simulations in common oncogenic drivers of leukemic and rhabdomyosarcoma cells: a systems biology approach. *Int J Oncol* 2012; 40:1365-90
- Cohen BA, Mitra RD, Hughes JD, Church GM. A computational analysis of whole-genome expression data reveals chromosomal domains of gene expression. *Nat Genet* 2000; 26:183-6; PMID:11017073; <http://dx.doi.org/10.1038/79896>
- Zaravinos A, Lambrou G, Boulalas I, Volanis D, Delakas D, Spandidos D. Linear Correlations in Chromosomal-Based Gene Expression in Urinary Bladder Cancer. *Urology* 2011; 78:S190
- Duggan BJ, McKnight JJ, Williamson KE, Loughrey M, O'Rourke D, Hamilton PW, et al. The need to embrace molecular profiling of tumor cells in prostate and bladder cancer. *Clin Cancer Res* 2003; 9:1240-7; PMID:12684390
- Dyrskjot L. Classification of bladder cancer by microarray expression profiling: towards a general clinical use of microarrays in cancer diagnostics. *Expert Rev Mol Diagn* 2003; 3:635-47; PMID:14510183; <http://dx.doi.org/10.1586/14737159.3.5.635>
- Dyrskjot L, Kruhoffer M, Thykjaer T, Marcussen N, Jensen JL, Møller K, et al. Gene expression in the urinary bladder: a common carcinoma in situ gene expression signature exists disregarding histopathological classification. *Cancer Res* 2004; 64:4040-8; PMID:15173019; <http://dx.doi.org/10.1158/0008-5472.CAN-03-3620>
- Dyrskjot L, Thykjaer T, Kruhoffer M, Jensen JL, Marcussen N, Hamilton-Dutoit S, et al. Identifying distinct classes of bladder carcinoma using microarrays. *Nat Genet* 2003; 33:90-6; PMID:12469123; <http://dx.doi.org/10.1038/ng1061>
- Modlich O, Prissack HB, Pitschke G, Ramp U, Ackermann R, Bojar H, et al. Identifying superficial, muscle-invasive, and metastasizing transitional cell carcinoma of the bladder: use of cDNA array analysis of gene expression profiles. *Clin Cancer Res* 2004; 10:3410-21; PMID:15161696; <http://dx.doi.org/10.1158/1078-0432.CCR-03-0134>
- Mor O, Nativ O, Stein A, Novak L, Lehavi D, Shibolet Y, et al. Molecular analysis of transitional cell carcinoma using cDNA microarray. *Oncogene* 2003; 22:7702-10; PMID:14576834; <http://dx.doi.org/10.1038/sj.onc.1207039>
- Sanchez-Carbayo M, Socci ND, Charytonowicz E, Lu M, Prystowsky M, Childs G, et al. Molecular profiling of bladder cancer using cDNA microarrays: defining histogenesis and biological phenotypes. *Cancer Res* 2002; 62:6973-80; PMID:12460915
- Sanchez-Carbayo M, Socci ND, Lozano JJ, Li W, Charytonowicz E, Belbin TJ, et al. Gene discovery in bladder cancer progression using cDNA microarrays. *Am J Pathol* 2003; 163:505-16; PMID:12875971; [http://dx.doi.org/10.1016/S0002-9440\(10\)63679-6](http://dx.doi.org/10.1016/S0002-9440(10)63679-6)
- Thykyjaer T, Workman C, Kruhoffer M, Demtröder K, Wolf H, Andersen LD, et al. Identification of gene expression patterns in superficial and invasive human bladder cancer. *Cancer Res* 2001; 61:2492-9; PMID:11289120
- Ying-Hao S, Qing Y, Lin-Hui W, Li G, Rong T, Kang Y, et al. Monitoring gene expression profile changes in bladder transitional cell carcinoma using cDNA microarray. *Urol Oncol* 2002; 7:207-12; PMID:12644218; [http://dx.doi.org/10.1016/S1078-1439\(02\)00192-8](http://dx.doi.org/10.1016/S1078-1439(02)00192-8)
- Lambrou GI, Vlachopoulos S, Papanthanasou C, Papanikolaou M, Karpusas M, Zoumakis E, et al. Prednisolone exerts late mitogenic and biphasic effects on resistant acute lymphoblastic leukemia cells: Relation to early gene expression. *Leuk Res* 2009; 33:1684-95; PMID:19450877; <http://dx.doi.org/10.1016/j.leukres.2009.04.018>
- Miyamoto H, Zheng Y, Izumi K. Nuclear hormone receptor signals as new therapeutic targets for urothelial carcinoma. *Curr Cancer Drug Targets* 2012; 12:14-22; PMID:22111835; <http://dx.doi.org/10.2174/156800912798888965>
- Kidokoro T, Tanikawa C, Furukawa Y, Katagiri T, Nakamura Y, Matsuda K. CDC20, a potential cancer therapeutic target, is negatively regulated by p53. *Oncogene* 2008; 27:1562-71; PMID:17873905; <http://dx.doi.org/10.1038/sj.onc.1210799>
- Huang C, Tang H, Zhang W, She X, Liao Q, Li X, et al. Integrated analysis of multiple gene expression profiling datasets revealed novel gene signatures and molecular markers in nasopharyngeal carcinoma. *Cancer Epidemiol Biomarkers Prev* 2012; 21:166-75; PMID:22068284; <http://dx.doi.org/10.1158/1055-9965.EPI-11-0593>
- Lee H, Kong SW, Park PJ. Integrative analysis reveals the direct and indirect interactions between DNA copy number aberrations and gene expression changes. *Bioinformatics* 2008; 24:889-96; PMID:18263644; <http://dx.doi.org/10.1093/bioinformatics/btn034>
- Cantile M, Franco R, Schiavo G, Procinio A, Cindolo L, Botti G, et al. The HOX genes network in uro-genital cancers: mechanisms and potential therapeutic implications. *Curr Med Chem* 2011; 18:4872-84; PMID:22050740; <http://dx.doi.org/10.2174/092986711797535182>
- Coskun U, Sancak B, Sen I, Bukan N, Tufan MA, Gülbahar O, et al. Serum P-selectin, soluble vascular cell adhesion molecule-I (s-VCAM-I) and soluble intercellular adhesion molecule-I (s-ICAM-I) levels in bladder carcinoma patients with different stages. *Int Immunopharmacol* 2006; 6:672-7; PMID:16504931; <http://dx.doi.org/10.1016/j.intimp.2005.10.009>
- Khin SS, Kitazawa R, Win N, Aye TT, Mori K, Kondo T, et al. BAMI gene is epigenetically silenced in subset of high-grade bladder cancer. *Int J Cancer* 2009; 125:328-38; PMID:19326429; <http://dx.doi.org/10.1002/ijc.24318>
- Tham SM, Ng KH, Pook SH, Esuvaranathan K, Mahendran R. Tumor and microenvironment modification during progression of murine orthotopic bladder cancer. *Clin Dev Immunol* 2011; 2011:865684; PMID:22013484; <http://dx.doi.org/10.1155/2011/865684>
- Rogala E, Skopi ska-Rózewska E, Sommer E, Pastewka K, Chorostowska-Wynimko J, Sokolnicka I, et al. Assessment of the VEGF, bFGF, aFGF and IL8 angiogenic activity in urinary bladder carcinoma, using the mice cutaneous angiogenesis test. *Anticancer Res* 2001; 21(6B):4259-63; PMID:11908679
- Oberbach A, Schlichting N, Blüher M, Kovacs P, Till H, Stolzenburg JU, et al. Palmitate induced IL-6 and MCP-1 expression in human bladder smooth muscle cells provides a link between diabetes and urinary tract infections. *PLoS ONE* 2010; 5:e10882; PMID:20526368; <http://dx.doi.org/10.1371/journal.pone.0010882>
- Clarke OW, Conley RB. The duty to "attend upon the sick". *JAMA* 1991; 266:2876-7; PMID:1942457; <http://dx.doi.org/10.1001/jama.1991.03470200088041>
- Jayasooriya RG, Choi YH, Moon SK, Kim WJ, Kim GY. Methanol extract of *Hydroclathrus clathratus* suppresses matrix metalloproteinase-9 in T24 bladder carcinoma cells by suppressing the NF- $\kappa$ B and MAPK pathways. *Oncol Rep* 2012; 27:541-6; PMID:21993858
- Zaravinos A, Lambrou GI, Volanis D, Delakas D, Spandidos DA. Spotlight on differentially expressed genes in urinary bladder cancer. *PLoS ONE* 2011; 6:e18255; PMID:21483670; <http://dx.doi.org/10.1371/journal.pone.0018255>
- Mengual L, Burset M, Ars E, Lozano JJ, Villavicencio H, Ribal MJ, et al. DNA microarray expression profiling of bladder cancer allows identification of noninvasive diagnostic markers. *J Urol* 2009; 182:741-8; PMID:19539325; <http://dx.doi.org/10.1016/j.juro.2009.03.084>
- Monzon FA, Lyons-Weiler M, Buturovic LJ, Rigl CT, Henner WD, Sciulli C, et al. Multicenter validation of a 1,550-gene expression profile for identification of tumor tissue of origin. *J Clin Oncol* 2009; 27:2503-8; PMID:19332734; <http://dx.doi.org/10.1200/JCO.2008.17.9762>
- Chandran UR, Ma C, Dhir R, Bisceglia M, Lyons-Weiler M, Liang W, et al. Gene expression profiles of prostate cancer reveal involvement of multiple molecular pathways in the metastatic process. *BMC Cancer* 2007; 7:64; PMID:17430594; <http://dx.doi.org/10.1186/1471-2407-7-64>
- Ramasamy A, Mondry A, Holmes CC, Altman DG. Key issues in conducting a meta-analysis of gene expression microarray datasets. *PLoS Med* 2008; 5:e184; PMID:18767902; <http://dx.doi.org/10.1371/journal.pmed.0050184>
- Sirbu A, Ruskin HJ, Crane M. Cross-platform microarray data normalisation for regulatory network inference. *PLoS ONE* 2010; 5:e13822; PMID:21103045; <http://dx.doi.org/10.1371/journal.pone.0013822>
- Klipper-Aurbach Y, Wasserman M, Braunsiegel-Weintrob N, Borstein D, Peleg S, Assa S, et al. Mathematical formulae for the prediction of the residual beta cell function during the first two years of disease in children and adolescents with insulin-dependent diabetes mellitus. *Med Hypotheses* 1995; 45:486-90; PMID:8748093; [http://dx.doi.org/10.1016/0306-9877\(95\)90228-7](http://dx.doi.org/10.1016/0306-9877(95)90228-7)
- Storey JD, Tibshirani R. Statistical significance for genome-wide studies. *Proc Natl Acad Sci USA* 2003; 100:9440-5; PMID:12883005; <http://dx.doi.org/10.1073/pnas.1530509100>

43. Storey JD, Tibshirani R. Statistical methods for identifying differentially expressed genes in DNA microarrays. *Methods Mol Biol* 2003; 224:149-57; PMID:12710672
44. Tritschler D, Parkhomenko E, Beyene J. Filtering genes for cluster and network analysis. *BMC Bioinformatics* 2009; 10:193; PMID:19549335; <http://dx.doi.org/10.1186/1471-2105-10-193>
45. Chartoumpakis DV, Zaravinos A, Ziros PG, Iskrenova RP, Psyrogiannis AI, Kyriazopoulou VE, et al. Differential expression of microRNAs in adipose tissue after long-term high-fat diet-induced obesity in mice. *PLoS one* 2012; 7:e34872
46. Zhang B, Schmoyer D, Kirov S, Snoddy J. GOTree Machine (GOTM): a web-based platform for interpreting sets of interesting genes using Gene Ontology hierarchies. *BMC Bioinformatics* 2004; 5:16; PMID:14975175; <http://dx.doi.org/10.1186/1471-2105-5-16>
47. Khatri P, Done B, Rao A, Done A, Draghici S. A semantic analysis of the annotations of the human genome. *Bioinformatics* 2005; 21:3416-21; PMID:15955782; <http://dx.doi.org/10.1093/bioinformatics/bti538>
48. Khatri P, Draghici S. Ontological analysis of gene expression data: current tools, limitations, and open problems. *Bioinformatics* 2005; 21:3587-95; PMID:15994189; <http://dx.doi.org/10.1093/bioinformatics/bti565>
49. Grossmann S, Bauer S, Robinson PN, Vingron M. Improved detection of overrepresentation of Gene-Ontology annotations with parent child analysis. *Bioinformatics* 2007; 23:3024-31; PMID:17848398; <http://dx.doi.org/10.1093/bioinformatics/btm440>
50. Bauer S, Grossmann S, Vingron M, Robinson PN. Ontologizer 2.0--a multifunctional tool for GO term enrichment analysis and data exploration. *Bioinformatics* 2008; 24:1650-1; PMID:18511468; <http://dx.doi.org/10.1093/bioinformatics/btn250>
51. Ashburner M, Ball CA, Blake JA, Botstein D, Butler H, Cherry JM, et al.; The Gene Ontology Consortium. Gene ontology: tool for the unification of biology. *Nat Genet* 2000; 25:25-9; PMID:10802651; <http://dx.doi.org/10.1038/75556>